GFD 2017 Lecture 10: Greenland Glacier–Ocean Interaction Part II

Fiamma Straneo; notes by Guillaume Michel and Madeleine Youngs

June 30, 2017

In this lecture, we detail the two-way coupling between the dynamics of glaciers and of the ocean: the melting of glaciers is caused by an inflow of warm seawater, that in return is cooled and freshened. This interaction affects the large-scale ocean dynamics, and is usually only considered as a boundary condition in numerical simulations.

In the first part of this lecture, we show how the melt rate can be evaluated. We then present how it is connected to the ocean dynamics.

1 How to estimate the melt rate?

For a given glacier, the melt rate depends on the characteristics of the water flow (*e.g.* temperature, salinity, vertical stratification and velocity). These properties set by the far-field ocean properties, but it remains challenging to infer a variation of the melt rate based on records in the ocean. This is a consequence of the large range of length-scales lying between an ice edge, a fjord, the nearby ocean, and the large-scale ocean currents, see Tab. 1.

Ice edge	Fjord	Nearby ocean	Far-field ocean
$L \sim 10 - 100$ m, $H \sim$ km	$W \sim 10$ km, $L \sim 100$ km	~ 100 km	~ 1000 km

Table 1: Typical length-scales involved in the glacier–ocean coupling. L stands for length, H for height, and W for width.

To estimate the melt rate, one can either:

1. For floating ice tongues, use the ice-flux divergence method, presented in the previous lectures. This method is recent and there is so far not enough data to investigate seasonal variability.

2. Perform a numerical simulation, and/or use a theoretical model. The thermal and salinity fluxes must then be characterized by transfer parameters (see *e.g.* equation (31) of lecture 5), whose values are not universal.

Since we lack data, we therefore lack an experimental way to estimate these fluxes. To fill this gap, we propose the *gate flux method*.

1.1 The gate flux method

1.1.1 General overview

Given that the width of a fjord is much smaller than its length, the large-scale dynamics of the water in this domain can be supposed to be uniform over the width. Therefore, local measurements of the water temperature, salinity and velocity with depth combined with conservation equations can be used to estimate the melt rate, see *e.g.* [1, 2, 3, 4].

For instance, the measurements of Inall *et al.* [4] performed in the calving front of Kangerdlugssuaq have been used to deduce that heat delivered by the warm water coming from the ocean is equivalent to a melt rate of $\sim 10\ \mathrm{m \cdot day^{-1}}$ (between 30% and 60% of the ice flux). The measurements, some of them being reported in Fig. 1, show a general feature of these exchanges:

1. Relatively hot water heads for the glacier below a few hundred meters.
2. Melting causes cooling, freshening and eventually upwelling (see Fig. 2 of Lecture 5).
3. Cold water leaves the Fjord near the surface.

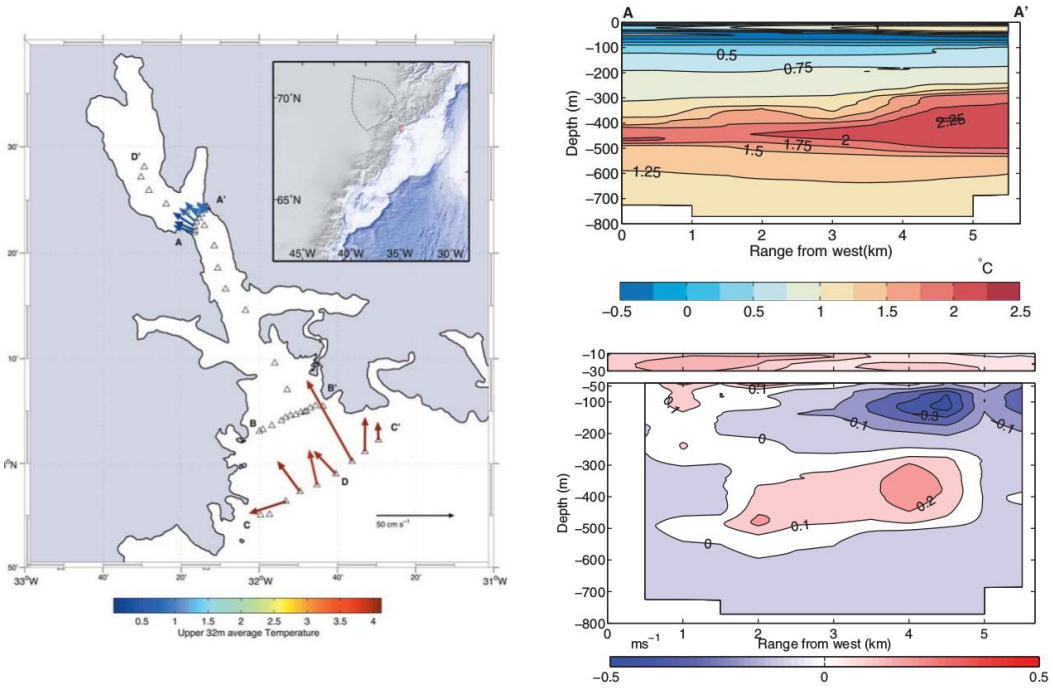

Figure 1: Left: schematic of the Kangerdlugssuaq Fjord, vector arrows represent upper velocity. Right: temperature and along-axis velocity across the measurement section AA'. Figures extracted from [4].

1.1.2 The underlying equations

In the gate flux framework, the complete heat, salt and mass budgets have been worked out by Jackson and Straneo [5]. Given the processes sketched in Fig. 2, they are as follows.

- Mass budget:

$$\int_{\mathcal{A}_x} u \mathrm{d}A + Q_\mathrm{R} + Q_\mathrm{MW} = 0, \tag{1}$$

  where u is the velocity perpendicular to the cross-section $\mathcal{A}_x$ (vertical left boundary of the control volume), Q_R is the runoff volume flux and Q_MW is the meltwater volume flux.

- Heat budget:

$$\rho c_\mathrm{p} \int_{\mathcal{A}_x} u\theta \mathrm{d}A + \rho c_\mathrm{p} Q_\mathrm{R} \theta_\mathrm{R} + \rho c_\mathrm{p} Q_\mathrm{MW} \theta_\mathrm{MW} + \rho c_\mathrm{p} Q_\mathrm{surf} \theta_\mathrm{surf} = \rho c_\mathrm{p} \frac{\partial}{\partial t} \int_\mathrm{V} \theta \mathrm{d}V + H_\mathrm{m} + H_\mathrm{s}, \tag{2}$$

  where the left-hand side terms stand for the advective heat flux through the control volume's boundaries (respectively : the cross-section $\mathcal{A}_x$, runoff, meltwater and surface). In the right-hand side, we identify the evolution of the properties of the control volume, the heat required to melt ice and the heat flux through the surface.

- Salt budget:

$$\int_{\mathcal{A}_x} uS \mathrm{d}A = \int_V \frac{\partial S}{\partial t} \mathrm{d}V, \tag{3}$$

  that balances advective transport through the section $\mathcal{A}_x$ with changes in the amount of salt stored in the control volume.

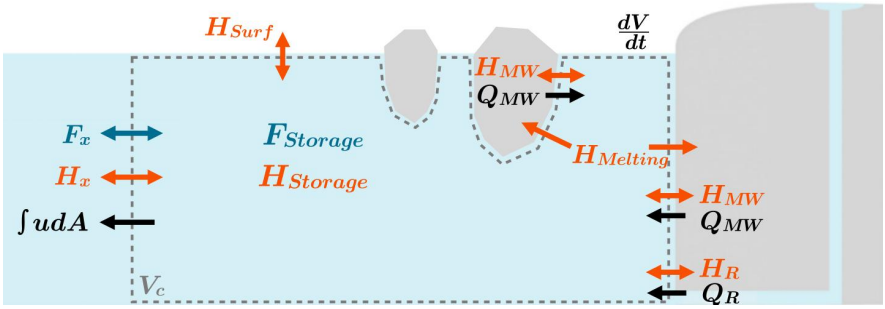

Figure 2: Control volume (grey dashed volume) and different processes taken into account. Figure extracted from [5].

For a practical use, time averaging as well as a differentiation between barotropic and baroclinic flow are useful. This leads to a new set of equations, see [5] for more details. Eventually, the mean meltwater volume flux, as well as other dominant fluxes, can be deduced from measurements.

1.1.3 Application to the Helheim glacier

The resulting set of equations is used to analyze measurements performed in the Sermilik Fjord, that connects to the Helheim Glacier. A satellite image is shown in Fig. 3, together with records of the water properties with time and depth. They strongly fluctuate, hence the need to distinguish between fast and slow time-scales.

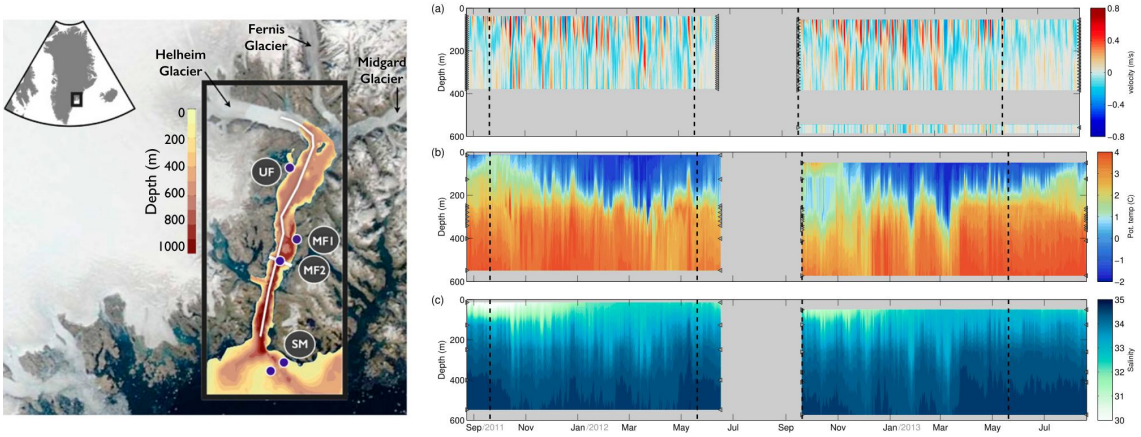

Figure 3: Left: sketch of the Sermilik Fjord. Right: velocity, potential temperature and salinity records at positions MF1 and MF2. Figure extracted from [5].

In winter, signal to noise ratio is low and freshwater fluxes do not appear c learly. On the other hand, in summer, the energy balance can be deduced and involves both the transported heat toward the glacier, storage in the water close to the glacier and melting.

Note that the melt rate deduced from these measurements includes icebergs melt, and thus differs from the melt rate of the glacier.

1.1.4 Application to an ice tongue

Exercise Consider the situation within the 79 North Cavity, sketched in Fig. 4, where Q_{in}, Q_{out} and S_{m} are the incoming, outgoing and melting volume fluxes, a nd T_{in} a nd T_{out} are the associated temperatures.

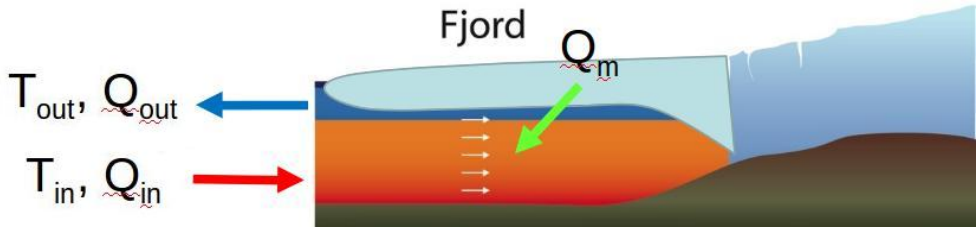

Figure 4: Exchanges with the 79 North Cavity.

Question: in a steady-state, give numerical estimates for Q_{in} and Q_{out}. Below are some numerical values that may be useful:

- The incoming temperature is $T_{\text{in}} = 1°\text{C}$.
- The outgoing temperature is $T_{\text{out}} = 0.2°\text{C}$.
- The temperature of ice is $T_{\text{i}} = -10°\text{C}$.
- The flux of meltwater is $Q_{\text{m}} = 0.36$ mSv. ($1\text{Sv} = 10^6\ \text{m} \cdot \text{s}^{-1}$)
- The heat capacity of ice is $c_{\text{i}} = 2\ \text{kJ} \cdot \text{kg}^{-1} \cdot \text{K}^{-1}$.
- The heat capacity of seawater is $c_{\text{w}} = 4\ \text{kJ} \cdot \text{kg}^{-1} \cdot \text{K}^{-1}$.
- The latent heat of fusion is $L_{\text{f}} = 334\ \text{kJ} \cdot \text{kg}^{-1}$.
- The density of ice is $\rho = 917\ \text{kg} \cdot \text{m}^{-3}$.

Solution: In a steady-state, the mass budget reads

$$Q_{\text{in}} = Q_{\text{out}} = Q_{\text{e}}, \tag{4}$$

with Q_{e} defined as the overturning exchange flow. The incoming heat balances the outgoing one and sustains the melting process,

$$Q_{\text{e}} \left(T_{\text{in}} - T_{\text{out}}\right) c_{\text{w}} = L_{\text{f}} Q_{\text{m}} \Longrightarrow Q_{\text{e}} = \frac{L_{\text{f}}}{c_{\text{w}}} \left(\frac{Q_{\text{m}}}{T_{\text{in}} - T_{\text{out}}}\right) = 38\ \text{mSv}. \tag{5}$$

See [6] for a detailed discussion of these water exchanges. Note that we ignore the heat required to raise the ice temperature from -10 $°C$ to 0 $°C$ because the latent heat is much higher than the heat capacity of ice.

1.2 Diagnosing meltwater and runoff concentrations

We thereafter present three methods that can be used to estimate both the meltwater and the runoff fluxes.

1.2.1 Using $T - S$ diagrams

As seen in a previous lecture, the melting of ice results, on a temperature-salinity diagram, in an evolution along a straight line toward the point $(T_{\text{eff}}, S_{\text{eff}})$ given in equation (5) of lecture 5.

Experimental measurements of the water properties at different depths may lie on this line (see the winter profiles in F ig. 5) or not (*e.g.* the summer measurements in F ig. 5). This deviation from the theoretical melting evolution indicates that another process is involved, namely the addition of run-off to ambient water. In this case, the addition of fresh run-off water at freezing temperature in the heat and salt budgets (equations (1) and (2) of lecture 5) can be used to deduce the run-off concentration from measurements.

For applications of this method, see *e.g.* [7, 8, 9].

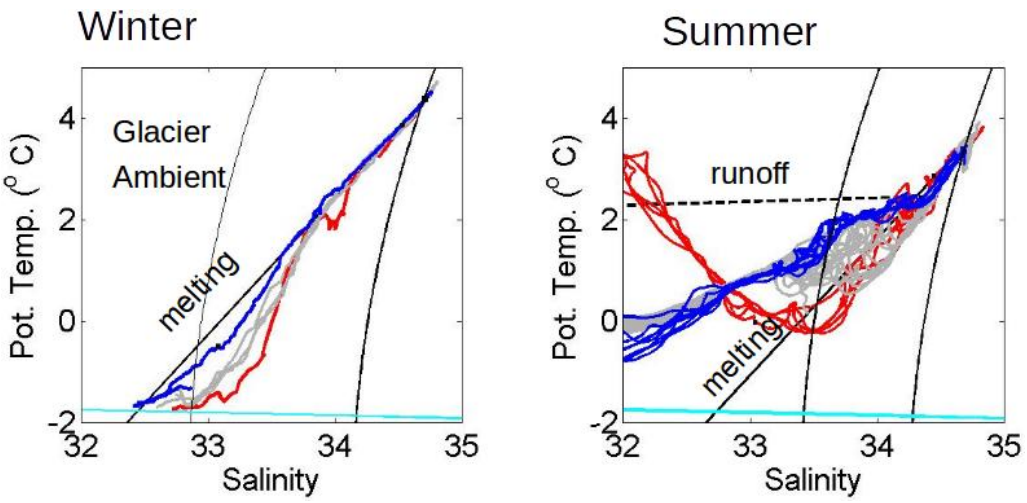

Figure 5: (T, S) diagram measurement in winter (left) and in summer (right) [7].

1.2.2 Using noble gases

Another method is based upon the non-uniform distribution of noble gases in seawater. Noble gases are inert and do not undergo chemical reactions: their concentrations only depend on the diffusive processes they have been through. Depending on the quantity of noble gas measured, it is therefore possible to distinguish between the different water origins:

- Surface melt runoff is formed at the surface of an ice sheet, is isolated and eventually melts into fresh water. The fraction of noble gas is then the one associated with solubility in fresh water at zero degree and one atmosphere.
- Submarine melt water, on the other hand, comes from melting under pressure, that results in anomalous noble gas concentration signals.

Examples of results than can be deduced from these measurements are reported in Fig. 6. We recognize the general structure of water fluxes close to a glacier, described in section 1.1.1, see [10] for an extensive discussion. This method has recently been used in the Sermilik fjord [11], to disentangle the subglacial discharge from the submarine melt, that turned out to be of similar amplitude.

1.2.3 Using nutrients

The upwelling of subglacial discharge and the entrained waters also results in an upwelling of nutrients, including nitrate, silicate and phosphate. They have been recently evidenced [12]. This provides an interesting information to discuss the biological life in a fjord. *A posteriori*, nutrients could also be used instead of noble gases.

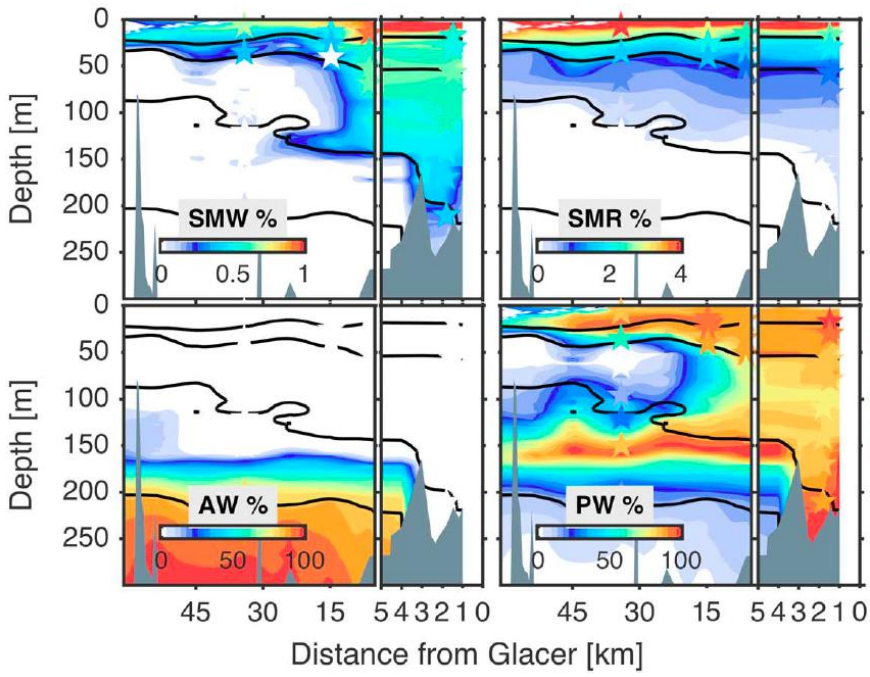

Figure 6: Extrapolation of the data to infer the distributions of submarine melt water (SMW), Antartic water (AW), surface melt runoff (SMR) and polar water (PW). Figure extracted from [10].

2 Ocean forcing by Greenland

There is clear evidence that freshwater fluxes from Greenland into the North Atlantic increase [13, 14, 15], which may have an impact on the ocean dynamics [16, 17, 18]. So far, ocean forcing by Greenland is taken into account through freshwater discharge conditions (see, *e.g.*, [15]), that are rough estimates and are not consistent with progress in ice/ocean exchanges. These difficulties in obtaining the freshwater flux partly come from icebergs.

2.1 Shortcomings in the current estimates of the freshwater flux

Consider the Sermilik Fjord, that consists of three glaciers and a significant catchment basin. A first approach to estimate the freshwater flux (FWF) consists of adding the discharge and the runoff fluxes, where:

- The discharge is obtained by adding the discharge of each of the three glaciers.
- The runoff is obtained by defining a catchment basin then by estimating the net melt from a regional climate models.

However, the freshwater flux evaluated this way differs from the freshwater flux at the fjord mouth, because of the transformation (my mixing) or delay (by storing) inside the fjord. Therefore, it is necessary either to resolve the dynamics at these small scales, which

is unrealistic for the current oceanic models, or to model this dynamics. This has been reviewed in [19], and we thereafter focus on the effect of icebergs. The calving of icebergs is necessary to balance the mass flux of a glacier when the melt rate from the glacier cannot remove enough mass.

2.2 Icebergs in fjords

2.2.1 Measurements from satellite images

Icebergs affect the FWF because they can either leave the fjord or melt in the fjord (some of this meltwater could then be trapped subsurface and/or affect the fjord circulation).

This solid ice flux has recently been estimated from satellite images and showed to dominate the freshwater budget in iceberg-congested glacial fjord [20]. Many properties of the icebergs can be deduced from satellite images (combined with models), such as the icebergs aspect ratio, size distribution and melt rates [21]. As can been seen in Fig. 7, the aspect ratio of iceberg is roughly constant ($W \simeq 2H$, where W is the width and H is the thickness), and the size distribution is self-similar. Similarly, the meltwater flux can be characterized as a function of the draft or as a function of the size of the dense matrix of floating ice [21].

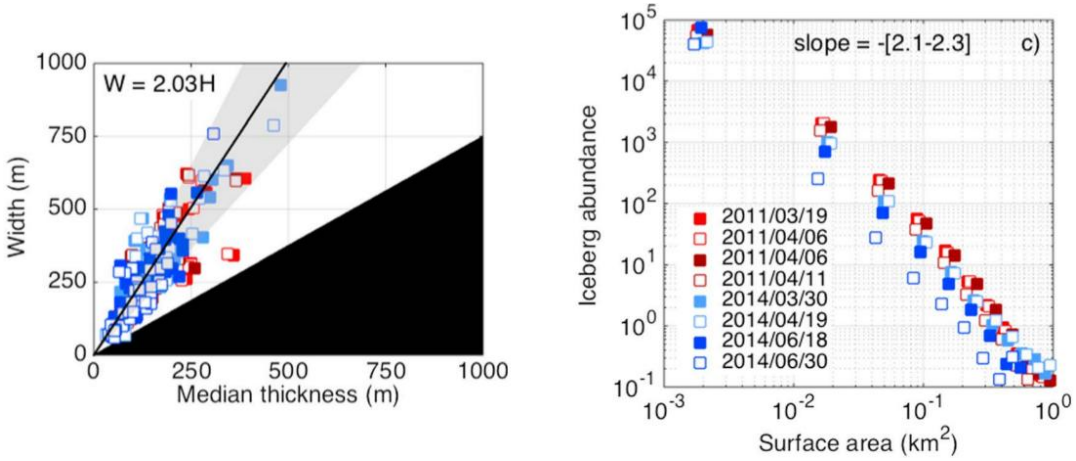

Figure 7: Icebergs ratio and size distribution for Ilulissat fjord. Figure extracted from [20].

2.2.2 In-situ measurements

Icebergs properties including draft and speed can also be measured using a inverted echo sounder at the bottom of the ocean [22]. This information gives us the mass flux of ice out of the domain and information about the freshwater budget. The current parameterizations of freshwater flux due to icebergs only use the surface velocities, but an iceberg actually travels using the vertical average of speeds along its draft, so we need better iceberg parameterizations to appropriately model the freshwater fluxes from glaciers [23].

2.2.3 Models of the iceberg melt flux

Models of iceberg melting are also used to examine the contribution of meltwater flux from icebergs [24]. This model includes a seasonality of the freshwater fluxes from icebergs due to changes in temperature distribution where the icebergs are melting (Fig. 8). Overall, there is more melting in the summer as expected, but the vertical distribution of the melting changes with the season and temperature distributions in the fjords.

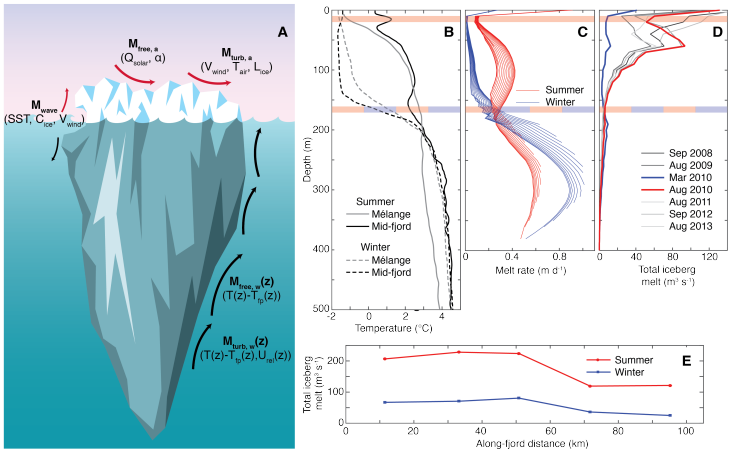

Figure 8: A figure showing the model of freshwater flux into ocean from icebergs. Figure extracted from [24].

This iceberg model is coupled with data to estimate the total freshwater flux into the ocean from the glacial system (Fig. 9). There is a large peak in the freshwater fluxes due to subglacial discharge in the summer months as the largest contribution. The second largest contribution is from iceberg melting which is lagged behind the subglacial discharge with a minimum in April and a maximum in September. The observations of iceberg melt agree well with the model where observations exist.

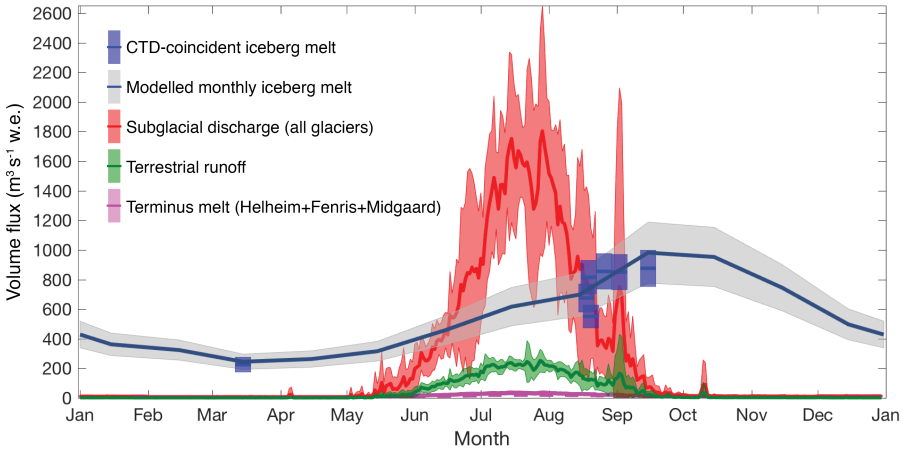

Figure 9: A figure showing the total freshwater flux into ocean throughout a year. Figure extracted from [24].

References

[1] R. Motyka *et al.* (2003) Submarine melting at the terminus of a temperate tidewater glacier, LeConte Glacier, Alaska, U.S.A., *Ann. Glaciol.* **36**, 57.

[2] E. Rignot *et al.* (2010) Rapid submarine melting of the calving faces of West Greenland glaciers. *Nat. Geosci.* **3**, 187.

[3] D. Sutherland and F. Straneo (2012) Estimating ocean heat transports and sumarine melt rates in Sermilik Fjord, Greenland, using lowered acoustic Doppler current profiler (ADCP) velocity profiles. *Ann. Glaciol.* **53**, 50.

[4] M. E. Inall *et al.*, (2014) Oceanic heat delivery via Kangerdlugssuaq Fjord to the southeast Greenland ice sheet. *J. Geophys. Res. Oceans* **119**, 631.

[5] R. H. Jackson and F. Straneo (2016) Heat, salt and freshwater budgets for a glacial fjord in Greenland. *J. Phys. Oceanogr.* **46**, 2735.

[6] N. J. Wilson and F. Straneo (2015) Water exchange between the continental shelf and the cavity of Nioghalvfjerdsbrae (79 North). *Geophys. Res. Lett.* **42**, 7648 (2015)

[7] F. Straneo (2011) Impact of fjord dynamics and glacial runoff on the circulation near Helheim Glacier. *et al.*, *Nat. Geosci.* **4**, 322.

[8] A. Jenkins (1999) The impact of melting ice on ocean waters. *J. Phys. Oceanogr.* **29**, 2370 (1999)

[9] H. G. Gade (1979) Melting of ice in sea water: A primitive model with application to the Antarctic ice shelf and icebergs. *J. Phys. Oceanogr.* **9**, 189.

[10] N. Beaird *et al.* (2015) Spreading of Greenland meltwaters in the ocean revealed by noble gases. *Geophys. Res. Lett.* **42**, 7705.

[11] N. Beaird *et al.*, in prep.

[12] Cape, M. *et al.*, in prep.

[13] T. W. N. Haine *et al.* (2015) Arctic freshwater export: Status, mechanisms, and prospects. *Global Planet. Change* **125**, 13.

[14] E. C. Carmack *et al.* (2016) Freshwater and its role i the Arctic marine system: Sources, disposition, storage, export, and physical and biogeochemical consequences in the Arctic and global oceans. *Geophys. Res. Bio.* **121**, 675.

[15] J. Bamber *et al.* (2012) Recent large increases in freshwater fluxes from Greenland into the North Atlantic. *Geophys. Res. Lett.* **39**, L19501.

[16] C. W. Böning *et al.*, (2016) Emerging impact of Greenland meltwater on deep-water formation in the North Atlantic Ocean. *Nat. Geosci.* **9**, 523.

[17] H. Luo *et al.* (2016) Oceanic transport of surface meltwater from the southern Greenland ice sheet. *Nat. Geosci.* **9**, 528.

[18] S. Rahmstorf *et al.*, (2015) Exceptional twentieth-century slowdown in Atlantic Ocean overturning circulation. *Nat. Clim. Change* **5**, 475.

[19] F. Straneo and C. Cenedese (2015) . The dynamics of Greenland's glacial fjords and their role in climate. *Ann. Rev. of Marine Sci.* **7**, 89.

[20] E. M. Enderlin *et al.* (2016) Iceberg meltwater fluxes dominate the freshwater budget in Greenland's iceberg-congested glacial fjords. *Geophys. Res. Lett.* **43**, 287.

[21] E. M. Enderlin and G. S. Hamilton (2014) Estimates of iceberg submarine melting from high-resolution digital elevation models: application to Sermilik Fjord, East Greenland. *J. Glaciol.* **60**, 1084.

[22] M. Andres *et al.* (2015) Icebergs and sea ice detected with inverted echo sounders. *J. Atmos. Oce. Tech.* **32**, 1042.

[23] A. FitzMaurice *et al.* (2016) Effect of a sheared flow on iceberg motion and melting. *Geophys. Res. Letters* **43** 12,520 (2016)

[24] Moon *et al.*, *Submitted*